CFD ANALYSIS AND OPTIMISATION OF TRIPLE VOLUTE EXIT DIFFUSER: VANED VS VANELESS AND VANE DESIGN

B. Dewar

(The Institute of Advanced Automotive Propulsion Systems, The University of Bath, United Kingdom, bd523@bath.ac.uk)

ABSTRACT

This work focuses on the CAD drafting, CFD analysis in ANSYS CFX and design optimisation using Optislang of a triple exit volute for a high speed centrifugal compressor. This work came about through a research project for a small high speed air compressor to drive the pneumatic systems of an electric bus.

A drafting method is detailed, the volute scroll cross section parametrised and the circumferential variation of volute cross section expressed in terms of hydraulic diameter. Different cross section variations are tested and an optimal one found with a mostly linear profile.

A CFD method is presented including mesh transforms and domain interfaces, a mesh convergence study is presented as well. Due to the high speed nature of the compressor the CFD method makes use of ramped functions in CEL (CFX Expression Language) for mass flow rate, RPM and time step.

Different hydraulic diameter vs circumferential position functions are tested for a vaneless diffuser of a nominal size. It was shown that a linear profile is best with a slight jump in size at the tongue. The volute profile selected was the one with the highest static pressure rise from the volute inlet to the average of the three volute outlets.

The selected volute profile was then tested with vaneless diffusers of different radii. It was shown that there exists an optimal radius between static pressure diffusion and total pressure drop, the one with the highest outlet static pressure was selected as optimal, in this case 1.375 times the impeller outlet radius.

A channel type diffuser vane was drafted and parametrised allowing for manipulation of its main features, such as wedge angle and vaneless space. The domain was sliced in order to allow for more efficient computation, this method was proven to reproduce acceptable results compared to a full simulation of all blade and volute passages.

A design database was generated allowing for the use of Optislang optimisation software. Response surfaces and correlation coefficient were determined between the vane input variables and the objective functions of static pressure rise and thermal efficiency. A gradient based method was used to find an optimal design. The optimal vane angle was 83 degrees, wedge angle of 3.46 degrees, the vane outer radius is 124% of the impeller outlet radius and the vanless space 10% of the impeller outlet radius.

The diffuser radius is re optimised with the addition of the diffuser vanes and shown that a smaller diffuser is optimal when vanes are added compared to a vaneless diffuser.

Finally, the vane number is adjusted and a final optimal vaned diffuser and volute reached. In this case the optimal vane number was 29, or 1.38 times the number of total impeller blades.

KEYWORDS
CFD, Compressor, Ansys CFX, Diffuser Vanes, Optimisation, Volute Design

NOMENCLATURE

This paper does not present too many mathematical formulations and any variables are generally well explained or presented within the text. However these variables are used:

R_i Impeller Exit Radius (m)
α Theoretical Flow Exit Angle (deg)
θ Vane Angle (deg)
ϕ Wedge Angle (deg)
b_h Blade Height at Impeller Exit (m)
ω Impeller Rotational Speed $\left(\frac{1}{s}\right)$
$\dot{m}$ Mass Flow Rate $(\frac{kg}{s})$
ρ_i Density at Impeller Exit $(\frac{kg}{m^3})$
D Impeller Outlet Diameter (m)

INTRODUCTION

At the heart of any high performing centrifugal compressor design is a well designed, and well matched, impeller and volute. There is a lot of literature, both from a CFD analysis and design optimisation point of view, with regard to the former, not so much the latter. For example, Younasi, et al. (2017) and Bardelli, et al (2019) give detail on commonly used CFD methods for impeller simulation, whilst Robinson, et al (2012) provide insight into impeller diffuser gap performance as well as rotor – diffuser blade number effects. These are all done with a single exit volute in mind.

Mojaddam, et al. (2012) presents a diffuser ratio (outlet to inlet radius ratio) of 1.3 and posits a method for varying the volute area circumferentially in a linear fashion, however this method assumes a low mach number.

Kim, et al. (2010) presents a larger diffuser ratio of 1.6 with a blade height comparable to the machine studied in this work. These two will inform the upper and lower bounds of the diffuser radius tested in this work.

Xu, (2007) shows that for a single exit volute the ideal circumferential variation of cross sectional area is slightly non linear.

There is some literature on how to best draft/draw the volute, particularly the cross section in Ansys Design Modeller, a commonly used package, such as in 'Mojaddam, et al. (2012)' This paper examines whether builds upon the existing volute cross sectional area variation using a triple exit volute and tests whether the commonly used diffuser length ratios for a single exit volute are

applicable to a multiple exit volute. Along the way aim of this work is to produce an optimised compressor-volute design and to examine the validity of use of domain slicing for the generation of an optimisation database.

This work provides a step by step approach to drafting, modelling, analysing and ultimately optimising the design of a multiple exit volute for a high speed centrifugal air compressor. The volute is drawn in Ansys design modeller, modelled in Ansys CFX and makes use of Optislang software for optimisation.

The key parameters investigated are volute profile shape, vaneless diffuser radius and diffuser vane shape.

THE IMPELLER

Whilst the impeller is not the main thrust of this paper an overview of it will be given here. The impeller is a high speed (on design speed 120 000 RPM) centrifugal compressor similar to Pakle, Jiang. (2018)

The required mass flow rate at design point was 0.04 kg/s and a static pressure ratio of 3.16 was required.

Meridional Profile

The impeller used is a shrouded impeller similar to that used in Younasi, et al. (2017) with an outlet radius of approximately 36mm and a blade outlet height of 1.75mm. The impeller exit mach number is in the range of 0.35, right on the edge of the compressible flow envelope. The extremities of the hub and shroud inlet and outlet in both axial (z) and radial (r) is given in Table 1. The impeller has 7 main blades and 2 splitter blades per blade channel, leading to 21 blades in total. The inlet hub radius was approximately 10% of the outlet hub radius, similar to the machine studied in Xu, Amano. (2012). The splitter blades were offset at one third and two thirds of the distance between each main blade, ie each blade is the same theta distance from the adjacent blade.

Table 1- Meridional Extremes

Location (r,z)	Hub	Shroud
Inlet	(3.5, 23.7)	(11.5, 23.7)
Outlet	(34.2, 0)	(34.2, 1.8)

Operating conditions

The compressor operating conditions are RPM = 120,000 and mass flow rate = 0.013 kg/s per volute exit (0.04 kg/s in total). Off design conditions are not considered. The target pressure ratio is 3.16 and the inlet conditions are total pressure inlet = 1 atm and total temperature inlet = 298 K

THE VOLUTE

The volute used in this work is a triple exit volute with a standard overhang scroll profile. The reason for the triple volute exit is that the compressor feeds a triple inlet intercooler which then feeds into the machine second compressor stage. The performance of a vaneless diffuser will be analysed first then diffuser vanes added to the optimised vaneless design.

The volute is comprised of three exits, each exit is comprised of a scroll whose size increases with circumferential variation and a volute exit of circular cross section. Each scroll profile is made up of

5 sketches at angles 0, 30, 60, 90 and 120 degrees. The exit starts at the final angle (120 degrees) and has the same shape as the final profile except that it does not include the diffuser. The sketches of one volute section are shown in Figure 1 and are highlighted in red. Profile_0 is in the same position as the proceeding Profile_120, hence it appears bigger than it actually is.

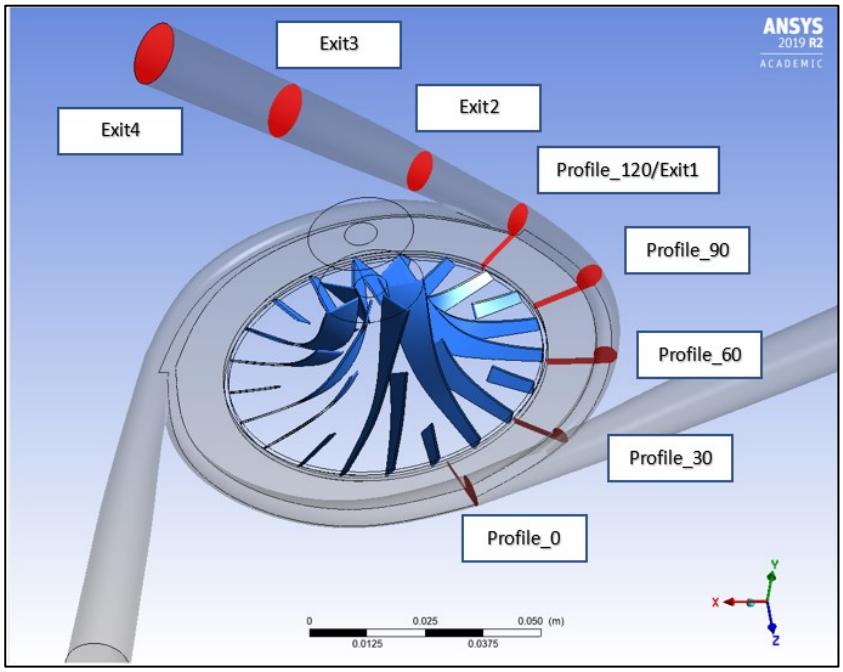

Figure 1: 3D Volute Profile Sketches Highlighted

Each volute section sketch follows the same shape but with different sizes. The profile is constructed by a rectangle representing the diffuser and an arc by three points to create the scroll profile. A typical section is shown in Figure 2. This shape is like that in Mojaddam, et al. (2012) except the inner part of the scroll has not been trimmed to the diffuser outlet radial value.

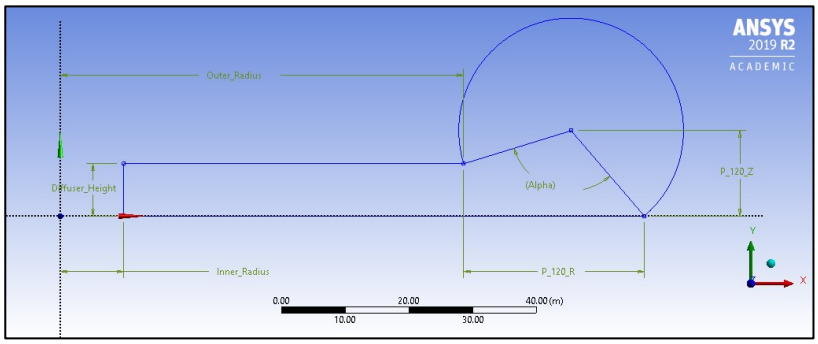

Figure 2 - Volute Profile Typical Section Sketch

The profile contains the following key parameters:

Inner_Radius = The radial distance from the axis of rotation to the diffuser inlet

Outer_Radius = The radial distance from the axis of rotation to the diffuser outlet

Diffuser_Height = The axial height of the diffuser

P_(theta)_R = The radial distance from the diffuser outlet to the outer point used in creating the arc for the scroll profile. In Figure 2 profile 120 degrees is shown, therefore the notation is P_120_R.

P_(theta)_Z = The axial distance from the diffuser hub outlet to the centre point used in creating the arc for the scroll profile. In Figure 2 profile 120 degrees is shown, therefore the notation is P_120_Z.

Alpha = This is a derived quantity and is the angle shown in Figure 2. Note that the lines shown do not exist in the actual model, they are shown for illustrative purposes.

Profile Shape and Hydraulic Diameter

Having established the base shape for each volute section it can be seen that the shape is not regular, per se. It was decided the best measure to quantify the profile shape was the hydraulic diameter. This is expressed as 4 times the area divided by the perimeter. The hydraulic diameter of each profile (excluding the diffuser) can be determined by recognising that an isosceles triangle can be formed inside the shape, together with some simultaneous equations the hydraulic diameter can be calculated just by the key parameters outlined above.

Volute Profiles

Having arrived at a profile shape and a method of quantifying its shape the next phase is to determine how to best change the shape of the volute as it progresses circumferentially. As hydraulic diameter is a function of both P_theta_R and P_theta_Z there is not one unique solution for a given hydraulic diameter. It was decided that P_theta_R was to increase linearly with circumferential angle.

Starting with a hydraulic profile shape, ie Hydraulic diameter as a function of circumferential angle, then assuming the P_theta_R start and end points one can use goal seek in MS Excel to work backwards and find the desired P_theta_Z.

Upwards of 20 different hydraulic diameter profiles were tested, a select few are shown in Figure 3. The performance metric used to evaluate the performance of the different volute shapes was the outlet static pressure, with the best performing profile being profile 11, which is represented by the solid line in Figure 3. The reason for the selection of overall static pressure rise is to try to encompass the coupled nature between the impeller and volute as best as possible and reflect the overall goal of the compressor. The results for the profiles shown in Figure 3 are shown in Figure 5.

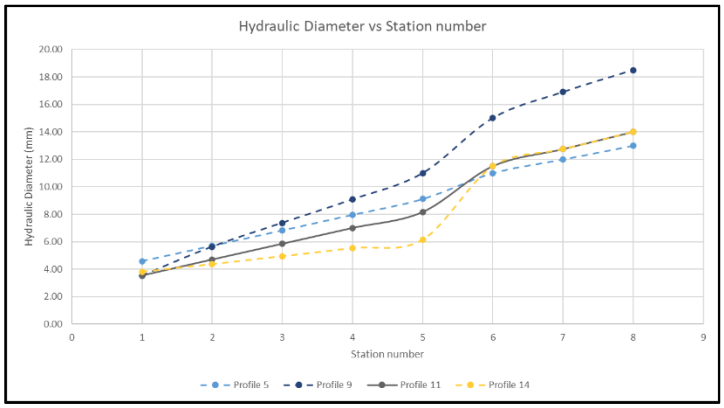

Figure 3 - Hydraulic Diameter Profiles

Where stations 1 to 5 represent circumferential position 0 to 120 degrees and stations 6 to 8 (exit 2 to 4 in Figure 1) represent the straight circular volute exit where Exit 1 is the same shape as Profile 120 but are kept separate for drafting reasons. Profile 11 shows that the ideal variation has a small non linear variation at the volute tongue.

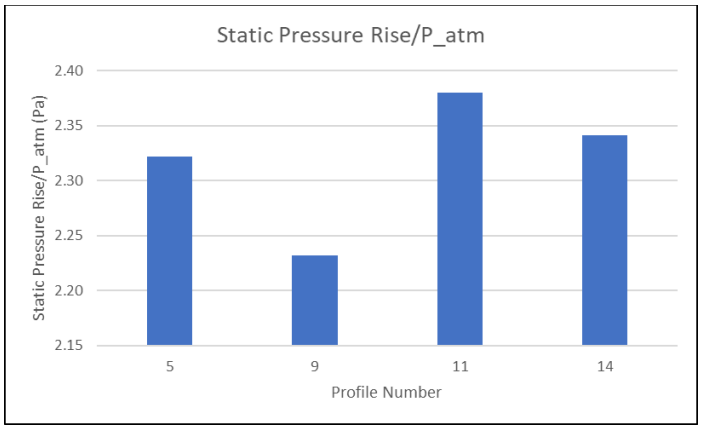

Figure 4: Static Pressure Rise in Different Volute Shapes

THE DIFFUSER VANES

Diffuser vanes are used to help improve flow uniformity and thus efficiency design operating point Tan, et al. (2016). The diffuser vanes are of the type used in channel diffusers and are of a triangular shape as in Robinson, et al. (2012) Tan, et al. (2016). The diffuser vanes were drawn in design modeller and their geometry parametrised. There are 5 main parameters concerning the diffuser vanes:

Vane Offset Radius = The radial offset the leading point of the vane has from the impeller exit, ie the vaneless space size. The minimum offset is 2% of impeller tip radius. This allows for the expected optimal gap of 9% shown in Robinson, et al. (2012) and 10% in Gibson, et al. (2018) to be investigated.

Vane angle = The vane offset angle from a purely radial line

Wedge angle = The angle of the vane wedge, ie the angle between the two vane edges

Outer Radius = The radius value of the line that cuts the vanes at their outer most point

Vane number = The number of vanes. The number of vanes should be circa 1.5 x the number of total compressor blades (main plus splitters) Bardelli, et al. (2019), Gibson, et al. (2018). Whereas Bai, et al. (2017) shows the best performance when vane number equals blade number + 1. Overall the number of vanes should be higher than the number of impeller blades and ideally both be prime numbers to prevent destructive interference.

The vanes ran the full height of the diffuser. This is for ease of manufacturing, modelling and best operating efficiency Zheng, et al. (2013). Initial simulations were run with the vane number = 38, or (38/21) = 1.8 x number of main plus splitter blades.

An illustrative sketch of the impeller, diffuser vanes and relevant velocity components is shown in Figure 5

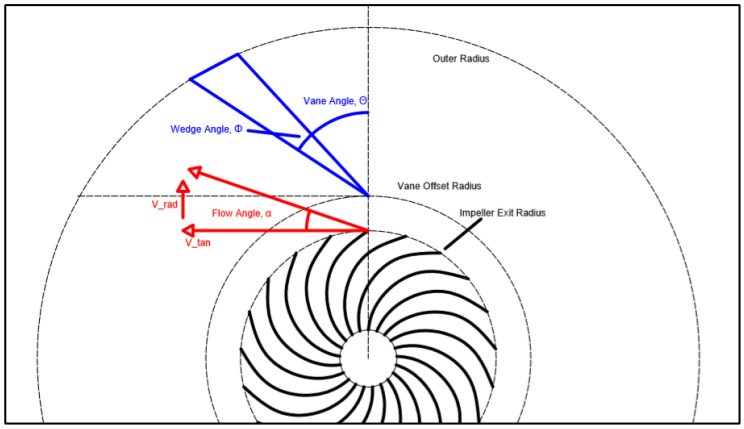

Figure 5 - Vane Sketch

In addition to the above listed variables Figure 5 also shows the theoretical tangential and radial velocity terms, these can be used to calculate the impeller exit flow angle. These are expressed as:

$$V_{tan} = 2\pi . R_i . \omega \qquad \text{Eqn [2]}$$

$$V_{rad} = \frac{\dot{m}}{\rho_i . 2\pi . b_h . R_i} \qquad \text{Eqn [3]}$$

$$\text{Theoretical Flow angle}, \alpha = \tan^{-1} \frac{V_{rad}}{V_{tan}} \qquad \text{Eqn [4]}$$

$$\text{Geometric Flow angle} = 90 - \text{vane angle} - \text{wedge angle} \qquad \text{Eqn [5]}$$

It is assumed the velocity direction remains constant from the impeller exit to vane inlet.

MESH SETUP

Mesh validation was done for the impeller, volute and diffuser vanes. The impeller mesh was validated separately and then the settled mesh setting used in the validation of the volute mesh settings. The volute simulated was vaneless. Once the settled impeller and vaneless volute settings were settled the diffuser vane mesh was tested. The volute the mesh was tested on was slightly different (such as in Figure 3) from the final design as mesh convergence was done before design optimisation. Values were non dimensionalised.

Impeller Mesh

The impeller was meshed using Turbogrid. Turbogrid contains pre set topology that allows for meshing of blade passages with two splitter blades. Boundary layer refinement was varied by using the factor base, factor ratio and global size factor. Total boundary layer refinement was tested between 1 and 5 producing results between 700,000 and 2,500,000 nodes. The y+ values in the passage were kept at 0.75 by selecting the appropriate option. The results of the convergence study are shown below in Figure 6.

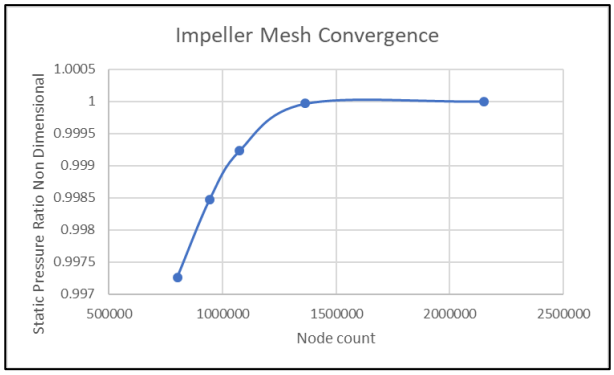

Figure 6 - Impeller Mesh Convergence

Volute Mesh

The volute was meshed using Ansys ICEM meshing. Named selections are utilised to impose sizing controls on various pieces of geometry. For example, line sizing is imposed on the Volute Inlet Hub line and the Volute Inlet Shroud line whilst face sizing is imposed on the Volute Inlet face and the Volute Shroud face. In addition, the mesh size and max size are also set. Key sizing can be shown in Figure 7. A mesh convergence study was also conducted for the volute mesh.

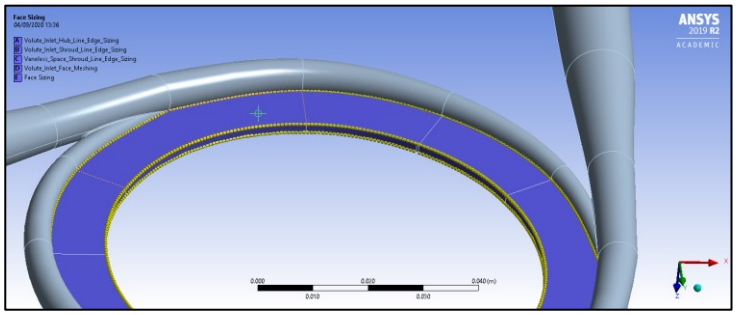

Figure 7 - Volute Mesh Line Sizing

Diffuser Vane Mesh

Named selections were used in design modeller to designate the edges of the diffuser vanes at the hub and shroud. This allowed to edge sizing to be used in the meshing process. The mesh size was the same as the volute inlet edge sizing as the diffuser height and vane length are of the same length scale.

CFD SETUP VANELESS DIFFUSER

The vaneless diffuser simulations were carried out using Ansys CFX v19R2. The computational domain (inlet, impeller and diffuser) for the impeller section is shown below in Figure 8.

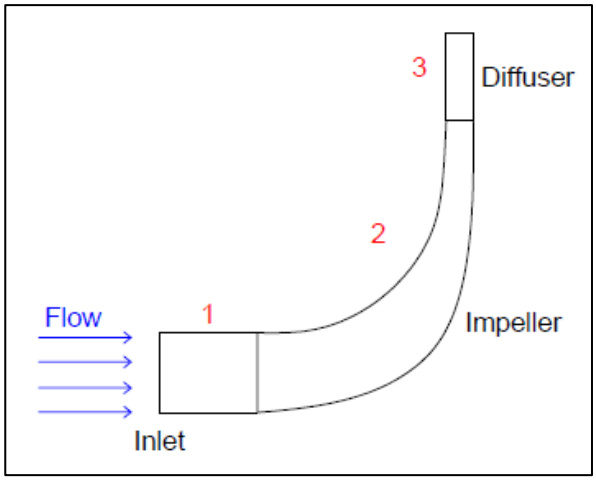

Figure 8 - Impeller Computational Domain

All blade passages (7 in total) were simulated by transforming the mesh in the setup cell to provide a one to one match with the volute inlet interface. The boundary conditions were:

Fluid = Air (project requirement), sub model = ideal gas Kalinkevycg, Skoryk. (2013).

Inlet = Total pressure (1 atm), Total temperature (298 K), Normal to boundary direction, Robinson, et al. (2012) Turbulence intensity (Medium 5%) Bardelli, et al. (2019)

Outlet = mass flow rate (0.013 kg/s) per volute outlet (3 in total) Robinson, et al. (2012)

Domain decomposition: The inlet (1), impeller(2) and a small part of the vaneless diffuser(3), such as used in Younasi, et al. (2017) were set as rotating. The volute scroll and the majority of the diffuser (vaned or vaneless) was modelled as one domain and set as stationary. A mixing reference frame interface such as in Younasi, et al. (2017) was placed between them. The walls of the inlet and vaneless diffuser in the rotating domain were set as counter rotating walls. This is to simulate their stationary nature without the need for interfaces between them and the rotating shrouded impeller. This contrasts with the method used in Tan, et al. (2016) and Gibson, et al. (2018) and eliminates the need for two interfaces.

Turbulence model = K Omega SST Younasi, et al. (2017) Robinson, et al. (2012) Bardelli, et al. (2019) as is suited for resolving adverse pressure gradients, heat transfer (Total Energy) Kalinkevycg, Skoryk. (2013), Viscous work and high speed wall heat transfer model turned on.

Numerics = Advection and turbulence numerics (High Resolution)

To aid in convergence the mass flow rate, RPM and time step were gradually changed using CEL boundary conditions. Without this the high speed nature of the machine meant convergence was not possible.

Time step = min(tstep, tstep_start*exp(tstep_Exponent*citern)

Mass flow rate = min(mdot, mdot_start*exp(mdot_exponent*citern)

RPM = min(RPM, RPM_start*exp(RPM_Exponent*citern)

Where citern is the current iteration number.

VANELESS DIFFUSER CFD RESULTS

The volute profile selected was the one with the highest static pressure rise and lowest total pressure drop from the volute inlet to the average of the three volute outlets.

Vaneless Diffuser Size Investigation

The settled profile design was then tested with varying diffuser lengths, from 1.25 to 1.67 times the impeller outlet radius, which is higher than the range specified in Robinson, et al. (2012). A minimum of 1.25 was selected to allow additional design freedom for the diffuser vanes. The criteria for performance assessment was the overall static pressure rise divided by atmospheric pressure. This was chosen to reflect the ultimate goal of the entire compressor: to increase the gas static pressure.

The results of this are shown in Figure 9.

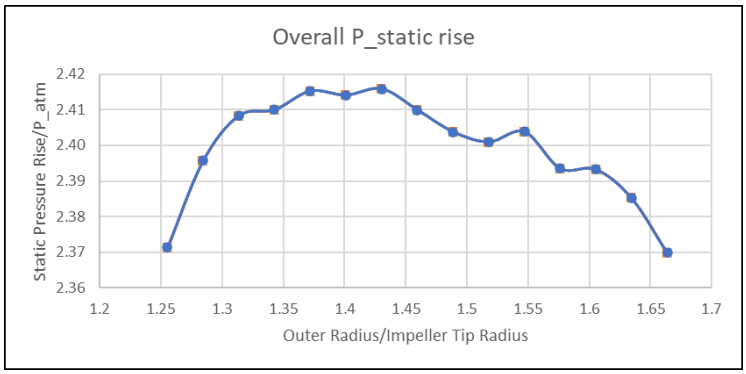

Figure 9 - Static Pressure Rise With Diffuser Radius: Vaneless Diffuser

From this it can be seen the optimal diffuser radius is approximately 1.37 times the impeller outlet tip radius. The final vaneless design produced an outlet pressure rise of 2.42 x atmospheric pressure at 73.8% thermal efficiency.

DOMAIN SLICE

Having arrived at an optimised vanless design the next step was to add vanes to the diffuser. The vanes are of a channel type, ie triangular shape, as opposed to vanes shaped more like an airfoil. In order to test more vane designs in a computationally efficient way the domain was sliced and periodic boundary conditions utilised. This method allowed for the computational time to be reduced by approximately 75% and thus a design database can be populated quicker.

The volute and diffuser was sliced so as to only simulate one outlet, ie 120 degrees. One impeller passage was simulated. The interface between the two had a pitch angle set: on the diffuser side it was (360/3) = 120 degrees, and on the impeller side it was 360/7 = 52 degrees approx. For both values an expression in CEL was defined so that both numbers were set exactly, as opposed to rounded decimal values. Periodic boundary conditions were applied at each end of the sliced diffuser and volute.

In order to determine where the domain should be sliced different cuts were investigated. 8 different slice locations were investigated, from 0 degrees to 60 degrees forward of the volute tongue. An illustration of the difference is shown in Figure 10.

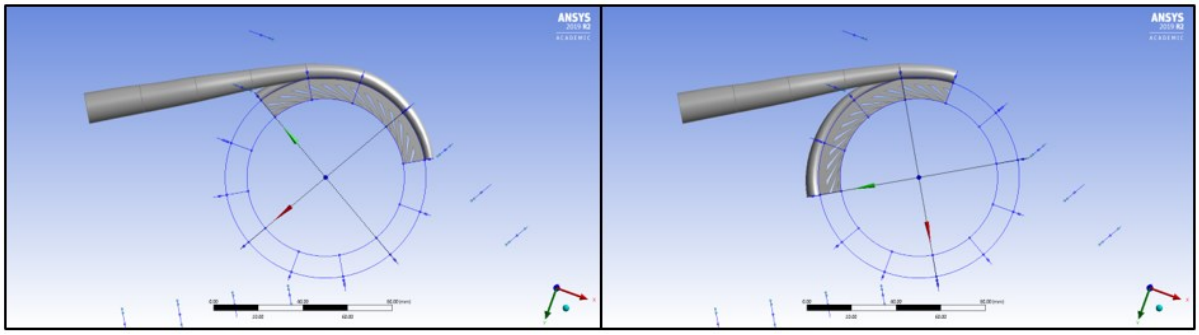

Figure 10 - Domain Slice at 0 and 60 Degrees Forward of Tongue

These results were then compared against the full annulus simulation and the results for total pressure showed the most accurate place to cut the domain is 22.5 degrees forward of the volute tongue where the outlet total pressure is approximately 98% that of the full annulus simulation.

CFD SETUP VANED DIFFUSER

The setup used for evaluating the vaned diffuser performance was identical as that used by the vaneless simulation except that to account for the domain slice a periodic boundary condition was applied at each sliced end of the volute, in the vaneless diffuser this is one single surface.

VANED DIFFUSER RESULTS

As mentioned in section 3 there are 5 input variables for the diffuser vanes. One, the vane number, will be treated individually once a final design has been settled. There are two objective functions considered: the outlet static pressure and the thermodynamic efficiency using static quantities. There are also 4 derived variables:

V_tan = Tangential velocity at vane inlet. This remains constant with constant RPM and impeller geometry

V_rad = Radial velocity at vane inlet.

These are needed to calculate:

Theoretical Flow angle, α = As defined in section 0.

Geometric flow angle = 90 – Vane Angle – Wedge Angle

Vane Outlet Radius/Diffuser Outlet Radius = For all vane designs all other geometric dimensions were kept constant, as such this is not fed into the optimiser, the vane outlet radius is, however this will come in further on. The range was 0.85 to 0.99.

The minimum and maximum values for vane and wedge angle, as well as the radial gap between the impeller exit and vane leading edge (vaneless space) and the vane outer radius, non dimensionalised against the impeller outlet radius are shown in Table 2 where Vane_OR = Vane outer radius, Imp_OR = Impeller outer radius, Rad_Off = Radial offset.

Table 2 - Vane Design Range

	Vane Angle	*Wedge Angle*	*Vane_OR/Imp_OR*	*Rad_Off/Imp_OR*
Min	*47.5*	*2*	*1.12*	*0.04*
Max	*83*	*11.3*	*1.31*	*0.15*

This shows the vaneless space results are between 3.65 and 15.3% of the impeller outer radius and the outer radius of the vanes is between 11.2 and 31.3% of the impeller outer radius.

In total approximately 150 designs were produced.

Response Surfaces

Using the optimisation software Optislang, mathematical meta models can be constructed that best model the input variables to the objective functions. These meta models include but are not limited to: Linear regression models, Moving least squares models and Kriging model. The MOP (Method of Optimal Prognosis) module considers all models for each input-output pair and selects the best one. Response surfaces can then be constructed to help visualise the data. For example, the effect the vane angle and wedge angle have on the outlet static pressure can be plotted. This is shown in Figure 11.

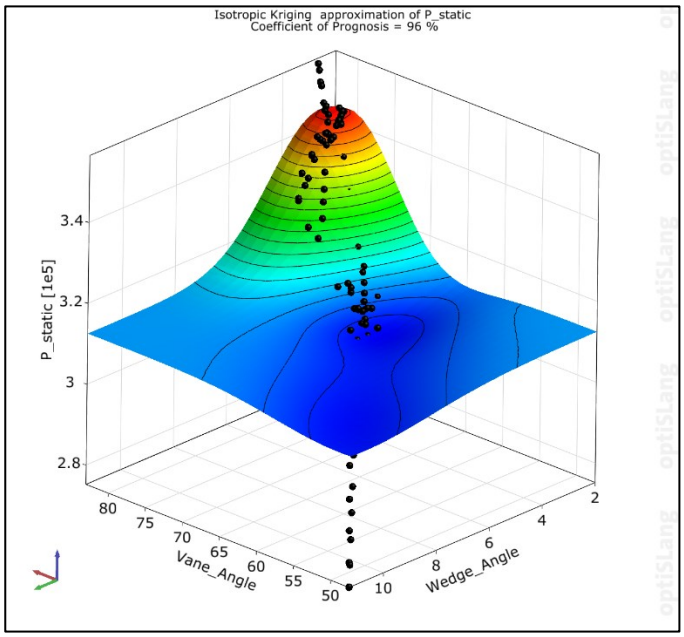

Figure 11 - Response Surfaces

Correlation Matrix

The MOP module also produces a matrix showing the correlation coefficient it's meta models have found between the input variables and objective functions. In this instance the MOP has assigned a correlation coefficient of -0.7 between Wedge Angle and Static Pressure outlet., ie a reasonably strong negative correlation between the two.

Geometric vs Theoretical Flow Angle

The difference between the geometric and theoretical flow angle also provided illuminating results. It was shown that the closer the two values are the higher the pressure outlet and efficiency. This is shown in Figure 12.

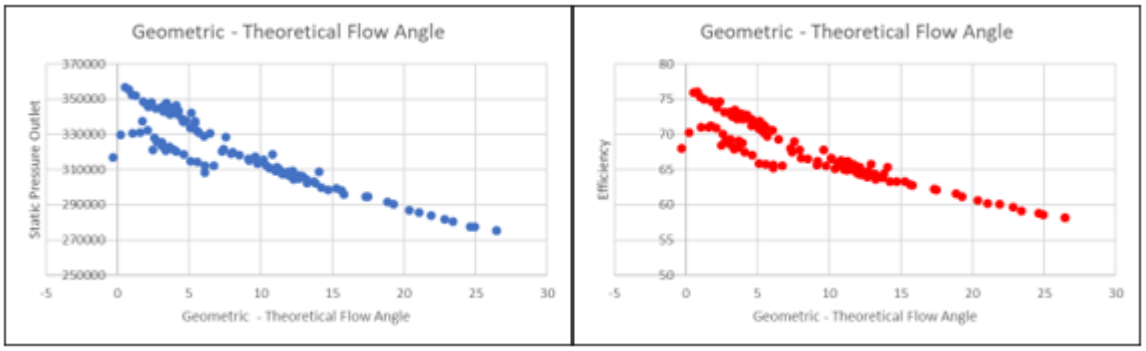

Figure 12 - Geometric Minus Theoretical Flow Angle

Optimised Design

The next step is to use the metamodels created in the MOP to optimise the design. In this instance the gradient based method NLPQL (Non linear programming quadratic lagrangian) was used. No constraints were applied on the input variables and the Efficiency objective function was to be maximised. The best design was selected as the starting design, this is the point at which the Optimiser begins exploring for an optimal design. The start design produced a static pressure outlet of 352500 Pa at an efficiency of 75.36%. The optimised design predicted at static pressure outlet of 358184 Pa at an efficiency of 76.71%. The optimised design was then run in CFD and produced an outlet static pressure of 367083 Pa at 78.81%, thus the optimiser under predicted the performance of the design. Adding this result back into the database and repeating the above process can continue to improve the final design. In this case the proven optimised design was well above required performance and so the process was stopped. The diffuser mid height static pressure contour is shown in Figure 13. For this design the difference between the theoretical and geometric flow angle was -0.9, confirming the correlation shown in Figure 12. The Vane Outlet Radius/Diffuser Outlet Radius for this design was 0.94. The vane angle was 83 degrees, wedge angle of 3.46 degrees, the vane outer radius is 124% of the impeller outlet radius and the vanless space 110% of the impeller outlet radius.

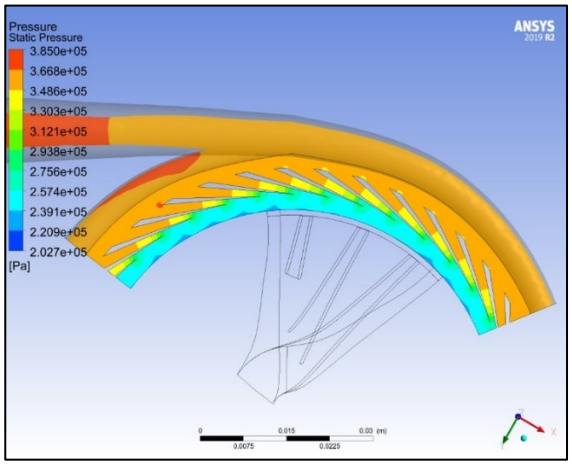

Figure 13 - Optimised Design Static Pressure Contour at Diffuser Mid Height.

Outer Radius Re-check

As outlined in earlier the optimal diffuser outer radius for a vaneless diffuser was 1.375 times the impeller outer radius. The addition of diffuser vanes is likely to impact this. With the optimal diffuser vane shape and the nominal vane number of 1.8 x number of main plus splitter blades the diffuser outer radius was varied, keeping the diffuser vanes size relative to the outer radius, for example the vane outlet radius was kept at 0.94 x the diffuser outlet radius. The results of this show that the addition of vanes has meant the optimal diffuser outer radius has been reduced to 1.34 x the impeller outer radius.

Vane Number

The final step in the process is to experiment with different vane numbers. The sliced domain used above can still be used as the gap between the vanes will remain the same. The optimal performance was found at diffuser vane number/ impeller blade number = 29/21. This achieved a marginal increase in efficiency from 78.81% to 79.36%. The results showed that more work is to be done on studying vane number, particularly with the initial theta offset w.r.t the volute tongue(s) and a more in depth look at convergence behaviour.

CONCLUSIONS

After outlining a suitable solution method and mesh convergence study this work netted some substantial insights for high speed turbomachinery design. The volute profile with respect to hydraulic diameter and circumferential variation was tested and an optimal profile found. An optimal vaneless diffuser design was achieved and showed the need for a balance between static pressure diffusion and total pressure losses. A diffuser vane shape was drawn and effectively parametrised in design modeller. A design database was then compiled more efficiently with the help of a domain slice method and periodic boundary conditions whereby the domain slice location was verified. Ansys Optislang was then used to present the data and shed light on the relative impact of each parameter on the objective functions of static pressure outlet and thermal efficiency. A gradient based optimisation method in Optislang was then used to optimise the diffuser vane geometry showing significant improvement in performance. It was also shown that the addition of diffuser vanes reduces the optimal diffuser outer radius. The diffuser vane number was investigated, and an optimal number found. Finally, the work raised questions regarding vane number, theta offset and convergence behaviour for different vane numbers.

REFERENCES

[1] Younasi, M., Corneloup, C., Baldacci, A. *"The Efficient Numerical Simulation of Unsteady Flow in a Centrifugal Compressor Stage Equipped with Vaned Diffuser",* Proceedings of the 12th European Conference on Turbomachinery Fluid Dynamics and Thermodynamics, Stockholm, Sweden, 2017

[2] Robinson, C., Hutchinson, B., Casey, M, *"Impeller - Diffuser Interaction in Centrifugal Compressors"*, Proceedings if ASME Turbo Expo 2012, Copenhagen, Denmark, 2012

[3] Bardelli, M., Cravero, C., Marini, M., Marsano, D., Milingi, O. *"Numerical Investigation of Impeller-Vaned Diffuser Interaction in a Centrifugal Compressor"*, Applied sciences Journal MDPI, 2019

[4] Y C Zheng, et al, *"Performance improvement of a centrifugal compressor stage by using different vaned diffusers"*, IOP Conference Series: Materials Science and Engineering, 2013

[5] Bai, Y., Kong, F., Xia, B., Liu, Y. *"Effect of blade number matching of impeller and diffuser in high speed rescue pump"*, Advances in Mechanical Engineering, 2017

[6] Kalinkevycg, M., Skoryk, A. *"Design method for channel diffusers of centrifugal compressors"*, International Journal of Rotating Machinery, 2013.

[7] Tan, MG., He, XH., Liu, HL., Dong, L., Wu,XF. *"Design and analysis of a radial diffuser in a single stage centrifugal pump"*, Engineering Applications of Computational Fluid Mechanics, 2016.

[8] Gibson, L., Spence, S., Kim, S.I., Schwitzke, M., Starke, A. *"A numerical investigation of a turbocharger compressor back disk cavity at widely operating conditions",* International Turbocharging seminar, 2018.

[9] Pakle, S., Jiang, K., *"Design of a high performance centrifugal compressor with new surge margin improvement technique for high speed turbomachinery",* Propulsion and power research, 2018.

[10] Xu, C., Amano, R. *"Empirical design considerations for industrial centrifugal compressors"*, International Journal of Rotating Machinery, 2012.

[11] Mojaddam, M., Benisi, A., Movahhedy, M., *"Investigation on the effect of centrifugal compressor volute cross section shape on performance and flow field",* Proceedings of ASME Turbo Expo, 2012.

[12] Kim, S., Park, S., Ahn, K., Baek, J. *"Improvement of the performance of a centrifugal compressor by modifying the volute inlet",* Journal of Fluids Engineering, 2010.

[13] Xu, C. *"Design experience and considerations for centrifugal compressor development",* Proceedings of the IMechE Vol 221 Part G: J. Aerospace Engineering, 2007.